

Synthesis, structure, magnetism and nuclease activity of tetranuclear copper(II) phosphonates containing ancillary 2,2'-bipyridine or 1,10-phenanthroline ligands†‡

Vadapalli Chandrasekhar,^{*a} Ramachandran Azhakar,^a Tapas Senapati,^a Pakkirisamy Thilagar,^a Surajit Ghosh,^a Sandeep Verma,^a Ramamoorthy Boomishankar,^b Alexander Steiner^b and Paul Kögerler^c

Received 21st August 2007, Accepted 16th November 2007

First published as an Advance Article on the web 7th January 2008

DOI: 10.1039/b712876b

The reaction of cyclohexylphosphonic acid (C₆H₁₁PO₃H₂), anhydrous CuCl₂ and 2,2'-bipyridine (bpy) in the presence of triethylamine followed by a metathesis reaction with KNO₃ afforded [Cu₄(μ-Cl)₂(μ₃-C₆H₁₁PO₃)₂(bpy)₄](NO₃)₂ (**1**). In an analogous reaction involving Cu(OAc)₂·H₂O, the complex [Cu₄(μ-CH₃COO)₂(μ₃-C₆H₁₁PO₃)₂(2,2'-bpy)₄](CH₃COO)₂ (**2**) has been isolated. The three-component reaction involving Cu(NO₃)₂·3H₂O, cyclohexylphosphonic acid and 2,2'-bipyridine in the presence of triethylamine afforded the tetranuclear assembly [Cu₄(μ-OH)(μ₃-C₆H₁₁PO₃)₂(2,2'-bpy)₄(H₂O)₂](NO₃)₃ (**3**). Replacing 2,2'-bipyridine with 1,10-phenanthroline (phen) in the above reaction resulted in [Cu₄(μ-OH)(μ₃-C₆H₁₁PO₃)₂(phen)₄(H₂O)₂](NO₃)₃ (**4**). In all the copper(II) phosphonates (**1–4**) the two phosphonate ions bridge the four copper(II) ions in a capping coordination action. Each phosphonate ion bridges four copper(II) ions in a μ₄, η³ coordination mode or 4.211 of the Harris notation. Variable-temperature magnetic studies on **1–4** reveal that all four complexes exhibit moderately strong intramolecular antiferromagnetic coupling. The DNA cleavage activity of complexes **1–4** is also described. Compounds **1** and **3** were able to completely convert the supercoiled pBR322 DNA form I to nick form II without any co-oxidant. In contrast, 50% conversion occurred with **2** and 40% with **4**. In the presence of magnesium monoperoxyphthalate all four compounds achieved rapid conversion of form I to form II.

Introduction

Transition metal phosphonates have been attracting considerable interest in recent years.¹ One of the reasons for this is the structural and compositional diversity that is present among these materials. In addition, they have also been attracting interest in view of their wide-ranging potential applications. These include their use as cation exchangers with potential utility in the processing of radioactive waste streams.² Other possible applications of these materials include sorption,³ catalysis,⁴ catalyst supports,⁴ sensors⁵ and nonlinear optics.⁶ Many transition metal phosphonates possess extended structures and are generally prepared by solvothermal and hydrothermal procedures. In recent years, there have also been efforts to prepare molecular phosphonates that are soluble in common organic solvents. One of the main challenges in this endeavour has been to devise new synthetic strategies. Use of sterically hindered and lipophilic phosphonic acids has been found to be conducive to promoting solubility.^{7–11} The use of phosphonic

acids in conjunction with ancillary ligands is another strategy that has gained importance for assembling discrete molecular assemblies of transition metal phosphonates.^{12–15} We have been interested, for some time, in developing appropriate synthetic routes for molecular main group and transition metal phosphonates.^{16–18} Our initial discovery of a lipophilic dodecanuclear copper phosphonate, [Cu₁₂(μ₄-Cl)₄(μ₃-Cl)₂(η¹-3,5-Me₂Pz)₆(η²-3,5-Me₂Pz)₄(μ₃-*t*-BuPO₃)₄(μ₂-*t*-BuPO₃)₂(μ₂-*t*-BuPO₂OH)₂ has spurred us to investigate the assembly and structures of molecular copper phosphonates. Previously we have shown that phosphonic acids (such as *t*-BuP(O)(OH)₂ or 2,4,6-*i*Pr₃-C₆H₂-PO₃H₂) in conjunction with ancillary ligands such as pyrazoles are extremely effective for the preparation of soluble molecular multi-metal phosphonates.^{19–21} In addition to the aforementioned dodecanuclear Cu(II) cage, we have also been able to isolate tetranuclear [Cu₄(μ₃-OH)₂{ArPO₂(OH)}₂(CH₃CO₂)₂(DMPZH)₄]-[CH₃COO]₂-CH₂Cl₂ (Ar = 2,4,6-*i*Pr₃-C₆H₂)²⁰ and decanuclear Cu(II) cages [Cu₅(μ₃-OH)₂(*t*-BuPO₃)₃(2-PyPz)₂(MeOH)]₂·10MeOH·2H₂O.²¹ In our quest for new lipophilic phosphonic acids we were intrigued by the possibility of using cyclohexylphosphonic acid as it satisfies the steric and lipophilic requirements. Although cyclohexylphosphonic acid has been known in the literature for quite some time, it has not been widely used for the preparation of molecular metal phosphonates. A cobalt(II) phosphonate, [Co(O₃PCy)·H₂O]_n and a cobalt complex [{Co(H₂O)₄(DMP)₂}-{CyPO₃H}₂]_n (DMP = 3,5-dimethylpyrazole; Cy = cyclohexyl) have been previously reported.²² However, the molecular structure of the former is unknown while the X-ray crystal structure

^aDepartment of Chemistry, Indian Institute of Technology Kanpur, Kanpur, UP, 208016, India. E-mail: vc@iitk.ac.in; Fax: +91 (0)512 259 7259

^bDepartment of Chemistry, University of Liverpool, Liverpool, U.K., L69 7ZD

^cAmes Laboratory and Department of Physics and Astronomy, Iowa State University, Ames, Iowa, 50011, USA

† CCDC reference numbers 641412–641415. For crystallographic data in CIF or other electronic format see DOI: 10.1039/b712876b

‡ Electronic supplementary information (ESI) available: MS spectra and selected bond angles and lengths for complexes **1–4**, with details of their supramolecular structures. See DOI: 10.1039/b712876b

of the latter showed that cyclohexylphosphonic acid is not coordinated to the metal ion but is present only as a counter anion. Herein we report the first (structurally characterized) examples of molecular transition metal phosphonates prepared by using cyclohexylphosphonic acid. Accordingly we describe in this paper the synthesis and molecular structures of tetranuclear copper(II) phosphonates $[\text{Cu}_4(\mu_3\text{-C}_6\text{H}_{11}\text{PO}_3)_2(\mu\text{-Cl})_2(\text{bpy})_4](\text{NO}_3)_2$ (**1**), $[\text{Cu}_4(\mu\text{-CH}_3\text{COO})_2(\mu_3\text{-C}_6\text{H}_{11}\text{PO}_3)_2(\text{bpy})_4](\text{CH}_3\text{COO})_2$ (**2**), $[\text{Cu}_4(\mu\text{-OH})(\mu_3\text{-C}_6\text{H}_{11}\text{PO}_3)_2(\text{bpy})_4(\text{H}_2\text{O})_2](\text{NO}_3)_3$ (**3**) and $[\text{Cu}_4(\mu\text{-OH})(\mu_3\text{-C}_6\text{H}_{11}\text{PO}_3)_2(\text{phen})_4(\text{H}_2\text{O})_2](\text{NO}_3)_3$ (**4**). We also report the magnetic properties and DNA cleavage activity of these compounds.

Experimental

Reagents and general procedures

Solvents were purified by conventional methods.²³ The following chemicals were used as received: $\text{C}_6\text{H}_{11}\text{Cl}$ (Aldrich, USA), $\text{Cu}(\text{OAc})_2 \cdot \text{H}_2\text{O}$ (Fluka, Switzerland), CuCl_2 (Lancaster, U.K.), 2,2'-bipyridine (Aldrich, U.S.A), 1,10-phenanthroline (Aldrich, U.S.A), AlCl_3 (s.d. Fine Chemicals, India), PCl_3 (s.d. Fine Chemicals, India) and $\text{Cu}(\text{NO}_3)_2 \cdot 3\text{H}_2\text{O}$ (s.d. Fine Chemicals, India). Supercoiled plasmid DNA (pBR322) was purchased from Bangalore Genei. Ethidium bromide was purchased from Sigma Aldrich Ltd. Magnesium monoperoxyphthalate hexahydrate (MMPP) was procured from Lancaster and was used as supplied, as was the sodium cacodylate buffer (SRL, Mumbai). Ethylenediaminetetraacetic acid (EDTA), DMSO, *tert*-butanol and D-mannitol were purchased from S.D. Fine Chemicals, Mumbai. All buffer solutions were prepared using Millipore water.

Instrumentation

Melting points were measured using a JSGW melting point apparatus and are uncorrected. Electronic spectra were recorded on a Perkin-Elmer Lambda 20 UV-Vis spectrometer and on a Shimadzu UV-160 spectrometer using methanol as the solvent. IR spectra were recorded as KBr pellets on a Bruker Vector 22 FT-IR spectrophotometer operating from 400–4000 cm^{-1} . ESI-MS analyses were performed on a Waters Micromass Quattro Micro triple quadrupole mass spectrometer. The ionization mechanism used was electrospray in positive ion full scan mode using methanol as solvent and nitrogen gas for desolvation. Capillary voltage was maintained at 3 kV and cone voltage was kept at 30 kV. The temperature maintained for the ion source was 100 °C and for desolvation was 250 °C. ^1H and $^{31}\text{P}\{^1\text{H}\}$ NMR spectra were recorded in CD_3OD solutions on a JEOL JNM LAMBDA 400 model spectrometer operating at 400.0 and 161.7 MHz respectively. Chemical shifts are reported in ppm and referenced with respect to internal tetramethylsilane (^1H) and external 85% H_3PO_4 (^{31}P). Elemental analyses were carried out using a Thermoquest CE Instruments CHNS-O, EA/110 model elemental analyzer.

Magnetic measurements

Magnetic susceptibility measurements were performed using a Quantum Design MPMS-5 SQUID magnetometer between a temperature range of 2–290 K and a field range of 0.1 to 5.0

tesla. Experimental DC susceptibility data have been corrected for diamagnetic contributions. Singlet ground states (and the absence of significant amounts of impurities such as isolated Cu(II) centres) were detected by field-dependent measurements. Least-squares fitting of the Heisenberg model Hamiltonian to the experimental data employed a modified version of MAGPACK.²⁴

pBR322 cleavage assay

Plasmid cleavage reactions were performed in sodium cacodylate buffer (10 mM, pH 7.5, 32 °C), containing pBR322 (8 ng μL^{-1} , Bangalore Genei), solution of the complexes **1–4** (1 mM) in distilled methanol and activating agents magnesium monoperoxyphthalate (MMPP, 100 μM). For each cleavage reaction, 16–18 μL of pBR322 supercoiled DNA, and 2 μL of complex **1–4** were used and they were initiated by adding 2 μL of magnesium monoperoxyphthalate in an Eppendorf tube. For scavenger experiments, concentrations used were 100 mM. All cleavage reactions were quenched with 5 μL of loading buffer containing 100 mM of EDTA, 50% glycerol in Tris–HCl, (pH 8.0) and the samples were loaded onto 0.7% agarose gel (Biozym) containing ethidium bromide (1 $\mu\text{g ml}^{-1}$). Electrophoresis was done for 1 h at constant current (80 mA) in 0.5 X TBE buffer. Gels were imaged with a PC-interfaced Bio-Rad Gel Documentation System 2000.

Plasmid cleavage under anaerobic conditions

Oxygen-free nitrogen was bubbled through cacodylate buffer, which was then subjected to four freeze–thaw cycles. All reagents were transferred in an argon-filled glove bag and Eppendorf tubes were tightly sealed with parafilm in the argon atmosphere. Reactions were quenched with loading buffer and efforts were made to ensure strict anaerobic conditions during irradiation and quenching.

Synthesis

$\text{C}_6\text{H}_{11}\text{P}(\text{O})(\text{OH})_2$. To a cooled mixture of AlCl_3 (10.0 g, 75.5 mmol) and PCl_3 (10.4 g, 75.7 mmol) at 0 °C, cyclohexylchloride (12.0 g, 101.2 mmol) was added slowly with stirring. After the addition, the reaction mixture became viscous. After standing overnight, 50 mL of CHCl_3 was added to this reaction mixture slowly with stirring at 0 °C. This was added to 150 g of ice and 30 mL of CHCl_3 . The organic portion was separated and dried over calcium chloride. It was filtered and the solvent evaporated from the filtrate to afford cyclohexylphosphonyl dichloride. To this, 30 mL of water was added and was stirred overnight. The solution was evaporated to dryness and the residue obtained was identified as impure cyclohexylphosphonic acid. This product was recrystallized from a 10 : 1 mixture of toluene and THF.

Yield: 9.94 g, 80.0% (based on phosphorus). Mp: 165 °C. FT-IR ν/cm^{-1} : 2934 (b), 2325 (b), 1451 (s), 1234 (m), 942 (m), 801 (m), 495 (m). ^1H NMR (CD_3OD): 1.15–1.86 (m). ^{31}P NMR (CD_3OD): 31.2 (s). ESI-MS analysis: m/z , ion: 165, $\{\text{M}+1\}^+$; anal. calc. for $\text{C}_6\text{H}_{13}\text{PO}_3$: C, 43.90; H, 7.98. Found: C, 43.76; H, 7.78.

$[\text{Cu}_4(\mu\text{-Cl})_2(\mu_3\text{-C}_6\text{H}_{11}\text{PO}_3)_2(\text{bpy})_4](\text{NO}_3)_2$ (1**)**. A mixture of anhydrous CuCl_2 (0.20 g, 1.5 mmol), 2,2'-bipyridine (0.24 g, 1.5 mmol), cyclohexylphosphonic acid (**1**) (0.13 g, 0.80 mmol) and triethylamine (0.36 g, 3.60 mmol) was taken in methanol (60 mL)

and stirred for 6 h. The blue coloured reaction mixture was filtered and treated with solid KNO_3 (0.08 g, 9.00 mmol). This mixture was stirred for further 3 h. The reaction mixture was filtered and the filtrate was stripped off the solvent *in vacuo* to afford a blue solid which was recrystallized from the methanol– CH_2Cl_2 solvent mixture to obtain the pure crystalline product.

Yield: 0.46 g, 88.5% (based on metal). Mp: 218 °C (d). UV-Vis (CH_3OH) $\lambda_{\text{max}}/\text{nm}$ ($\epsilon/\text{L mol}^{-1} \text{cm}^{-1}$): 695 (186). FT-IR ν/cm^{-1} : 3430 (b), 2928 (s), 2675 (s), 2675 (m), 2494 (s), 1604 (m), 1382 (m), 1070 (m), 776 (m), 575 (m). ESI-MS: m/z , ion: 637, $[\text{Cu}_2(\text{Cl})(\text{C}_6\text{H}_{11}\text{PO}_3)(\text{bpy})_2]^+$. Other peaks are observed at 150, 254, 382, 410, 546, 673, 763, 801 and 927. Anal. calc. for $\text{C}_{52}\text{H}_{54}\text{N}_{10}\text{P}_2\text{O}_{12}\text{Cu}_4\text{Cl}_2$: C, 44.67; H, 3.89; N, 10.02. Found: C, 44.37; H, 3.76; N, 10.10.

$[\text{Cu}_4(\mu\text{-CH}_3\text{COO})_2(\mu_3\text{-C}_6\text{H}_{11}\text{PO}_3)_2(\text{bpy})_4](\text{CH}_3\text{COO})_2$ (2). A mixture of copper(II) acetate monohydrate (0.20 g, 1.00 mmol), 2,2'-bipyridine (0.16 g, 1.00 mmol), cyclohexylphosphonic acid (0.08 g, 0.50 mmol) and triethylamine (0.22 g, 2.17 mmol) were taken in methanol (60 mL) and stirred for 6 h. The blue coloured reaction mixture was filtered and the filtrate was evaporated to afford a blue coloured solid. This was recrystallized from a mixture of methanol–ethanol (1 : 1) to get a pure crystalline product.

Yield: 0.28 g, 79.8% (based on metal). Mp: 120 °C (d). UV-Vis (CH_3OH) $\lambda_{\text{max}}/\text{nm}$ ($\epsilon/\text{L mol}^{-1} \text{cm}^{-1}$): 668 (180). FT-IR ν/cm^{-1} : 3387 (b), 1613 (m), 1446 (m), 1260 (s), 1165 (s), 1080 (m), 779 (s), 672 (s), 585 (s). ESI-MS: m/z , ion: 659, $[\text{Cu}_2(\text{CH}_3\text{COO})(\text{C}_6\text{H}_{11}\text{PO}_3)(\text{bpy})_2]^+$. Other peaks are observed at 150, 278, 375, 431, 492, 565, 763 and 886. Anal. calc. for $\text{C}_{60}\text{H}_{66}\text{N}_8\text{O}_{14}\text{P}_2\text{Cu}_4$: C, 50.07; H, 4.62; N, 7.79. Found: C, 49.60; H, 4.32; N, 7.56.

$[\text{Cu}_4(\mu\text{-OH})(\mu_3\text{-C}_6\text{H}_{11}\text{PO}_3)_2(\text{bpy})_4(\text{H}_2\text{O})_2](\text{NO}_3)_3$ (3). A mixture of copper(II) nitrate trihydrate (0.18 g, 0.75 mmol), 2,2'-bipyridine (0.11 g, 0.70 mmol), cyclohexylphosphonic acid (1) (0.06 g, 0.35 mmol) and triethylamine (0.15 g, 1.48 mmol) were taken in methanol (60 mL) and stirred for 6 h. The blue coloured reaction mixture was filtered and the filtrate was evaporated to afford a blue coloured solid. This was recrystallized from a mixture of methanol–ethanol to get a pure crystalline product.

Yield: 0.18 g, 67.0% (based on metal). Mp: 236 °C (d). UV-Vis (CH_3OH) $\lambda_{\text{max}}/\text{nm}$ ($\epsilon/\text{L mol}^{-1} \text{cm}^{-1}$): 677 (226). FT-IR ν/cm^{-1} : 3431 (b), 2927 (m), 1605 (m), 1359 (m), 1104 (m), 774 (s), 732 (s), 696 (s), 582 (m). ESI-MS: m/z , ion: 889, $[\text{Cu}_3(\text{C}_6\text{H}_{11}\text{PO}_3)(\text{OH})_3(\text{H}_2\text{O})(\text{bpy})_3]^+$. Other peaks are observed at 492, 637, 662, 765, 793 and 1045. Anal. calc. for $\text{C}_{52}\text{H}_{59}\text{N}_{11}\text{P}_2\text{O}_{18}\text{Cu}_4$: C, 43.31; H, 4.12; N, 10.68. Found: C, 43.10; H, 3.98; N, 10.36.

$[\text{Cu}_4(\mu\text{-OH})(\mu_3\text{-C}_6\text{H}_{11}\text{PO}_3)_2(\text{phen})_4(\text{H}_2\text{O})_2](\text{NO}_3)_3$ (4). A mixture of copper(II) nitrate trihydrate (0.18 g, 0.70 mmol), 1,10-phenanthroline (0.13 g, 0.70 mmol), cyclohexylphosphonic acid (0.06 g, 0.35 mmol) and triethylamine (0.15 g, 1.48 mmol) were taken in methanol (60 mL) and stirred for 6 h. The blue coloured reaction mixture was filtered and the filtrate was evaporated to afford a blue coloured solid. This was recrystallized from a mixture of methanol–ethanol to get a pure crystalline product.

Yield: 0.17 g, 59.3% (based on metal). Mp: 238 °C (d). UV-Vis (CH_3OH) $\lambda_{\text{max}}/\text{nm}$ ($\epsilon/\text{L mol}^{-1} \text{cm}^{-1}$): 683 (225). FT-IR ν/cm^{-1} : 3424 (b), 2924 (m), 1623 (m), 1372 (m), 1214 (s), 1133 (m), 854 (s), 725 (s), 647 (m), 578 (m). ESI-MS: m/z , ion: 1117, $[\text{Cu}_3(\text{C}_6\text{H}_{11}\text{-}$

$\text{PO}_3)_2(\text{NO}_3)(\text{C}_{12}\text{H}_8\text{N}_2)_3]^+$. Other peaks are seen at 406, 516, 528, 679, 710, 811, 937. Anal. calc. for $\text{C}_{60}\text{H}_{59}\text{N}_{11}\text{P}_2\text{O}_{18}\text{Cu}_4$: C, 46.85; H, 3.87; N, 10.02. Found: C, 46.65; H, 3.78; N, 9.96.

X-Ray crystallography†

The crystal data and the parameters for the compounds (1–4) are given in Table 1. Single crystals of 1, suitable for X-ray crystallographic analysis, were obtained by slow evaporation of a dichloromethane and methanol (1 : 1) solution at room temperature. Crystals of 2–4 were obtained by slow evaporation of their methanolic solutions. The crystal data for 1, 2 and 4 were collected on a Stoe-IPDS machine while those for 3 were obtained on a Bruker SMART APEX CCD Diffractometer. All structures were solved by direct methods using the programs SHELXS-97 and refined by full-matrix least-squares methods against F^2 with SHELXL-97.²⁵ All non-hydrogen atoms were refined with anisotropic displacement parameters. Hydrogen atoms were included at idealized positions and refined isotropically. The crystals of 3 are poor and weakly diffracting at 2θ above 50° and hence these reflections are omitted. The structure contains large solvated nitrate and water molecules. Although the electron densities in the solvated regions are overlapping each other, we were able to locate all the nitrate positions. Out of the six nitrate molecules four of them are present in two different positions (N50, N60, N70 and N80 sets) and one of them (N40 set) is in an inversion centre and is refined with half occupancies. The other high electron density peaks are carefully examined and are assigned as full or disordered water molecules. Restraining some of these water positions as nitrates did not refine well and hence assigning them as waters (with the aid of possible meaningful H-bonding patterns) gives the best model for refinement. The amount of disorder present in these solvated regions did not allow us to locate the hydrogen atoms on the water molecules. Some of the carbons and nitrogens of the 2,2'-bipyridine are disordered as observed from their slightly large thermal ellipsoids, but refining them anisotropically gives a more stable refinement than isotropically refining them in two different positions. The crystals of the compound 2 diffracted very poorly, displaying broad and weak reflections. Measured intensities therefore have a high $\sigma(I)$. As a consequence, R_{int} for this is relatively high.

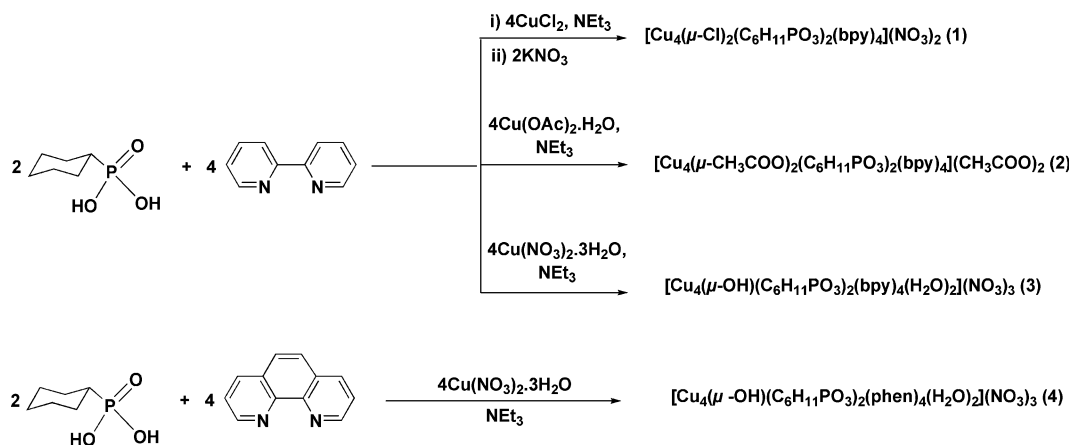
Results and discussion

Synthesis

The synthesis of the tetranuclear copper(II) complexes (1–4) using cyclohexylphosphonic acid and chelating nitrogenous ligands (bpy and phen) is shown in Scheme 1. In spite of the fact that these are three-component reactions involving a metal ion and two independent ligands, in each case, the isolated yields are quite good and range from 59.3% (4) to 88.5% (1) (*vide supra*, Experimental). Complexes 1–2 contain a tetranuclear dicationic part with nitrate or acetate counter anions, while complexes 3–4 are tricationic with nitrate counter anions (Chart 1). In each case, the synthesis was carried out such that every copper is chelated with one bidentate bpy or phen ligand. All four complexes are held together by the tridentate coordination mode of the two phosphonate ligands

Table 1 Crystal and structure refinement parameters for compounds 1–4

Parameters	1	2	3	4
Empirical formula	C ₃₆ H ₆₂ Cl ₁₀ Cu ₄ N ₁₀ O ₁₂ P ₂	C ₆₂ H ₇₄ Cu ₄ N ₈ O ₁₈ P ₂	C ₅₂ H ₇₁ Cu ₄ N ₁₁ O ₂₄ P ₂	C ₆₀ H ₆₅ Cu ₄ N ₁₁ O ₂₁ P ₂
Formula weight	1737.76	1535.39	1514.27	1592.33
Temperature/K	213(2)	213(2)	100(2)	213(2)
Wavelength/Å	0.71073	0.71073	0.71073	0.71073
Crystal system	Triclinic	Monoclinic	Triclinic	Monoclinic
Space group	<i>P</i> -1	<i>P</i> 2(1)/ <i>c</i>	<i>P</i> -1	<i>C</i> 2/ <i>c</i>
Unit cell dimensions (lengths in Å, angles in °)	<i>a</i> = 10.762(3) <i>b</i> = 12.649(4) <i>c</i> = 14.253(4) <i>a</i> = 67.88(3) <i>β</i> = 72.84(2) <i>γ</i> = 84.47	<i>a</i> = 11.747(3) <i>b</i> = 17.734(4) <i>c</i> = 18.981(5) <i>a</i> = 90 <i>β</i> = 104.22(3) <i>γ</i> = 90	<i>a</i> = 13.3151(10) <i>b</i> = 15.0690(11) <i>c</i> = 32.232(2) <i>a</i> = 81.051(10) <i>β</i> = 87.441(10) <i>γ</i> = 78.351(10)	<i>a</i> = 24.125(5) <i>b</i> = 15.624(2) <i>c</i> = 18.860(4) <i>a</i> = 90 <i>β</i> = 106.76(2) <i>γ</i> = 90
Volume/Å ³ , <i>Z</i>	1717.2(8), 1	3832.9(15), 2	6256.4(8), 4	6807(2), 4
Density (calculated)/mg m ⁻³	1.680	1.330	1.608	1.554
Absorption coefficient/mm ⁻¹	1.723	1.202	1.478	1.361
<i>F</i> (000)	880	1584	3112	3264
Crystal size/mm	0.1 × 0.2 × 0.1	0.2 × 0.3 × 0.2	0.2 × 0.2 × 0.2	0.1 × 0.1 × 0.1
<i>θ</i> range for data collection/°	1.89 to 24.27	4.10 to 22.49	4.09 to 25.03	4.10 to 22.49
Limiting indices	−11 ≤ <i>h</i> ≤ 12, −14 ≤ <i>k</i> ≤ 14, −16 ≤ <i>l</i> ≤ 16	−12 ≤ <i>h</i> ≤ 12, −19 ≤ <i>k</i> ≤ 19, −20 ≤ <i>l</i> ≤ 20	−15 ≤ <i>h</i> ≤ 15, −17 ≤ <i>k</i> ≤ 17, −38 ≤ <i>l</i> ≤ 38	−25 ≤ <i>h</i> ≤ 25, −16 ≤ <i>k</i> ≤ 16, −20 ≤ <i>l</i> ≤ 20
Reflections collected	10919	19870	46469	15756
Independent reflections	5117 (<i>R</i> _{int} = 0.0747)	4978 (<i>R</i> _{int} = 0.1674)	21846 (<i>R</i> _{int} = 0.0245)	4429 (<i>R</i> _{int} = 0.0702)
Completeness to <i>θ</i> (%)	91.7 (<i>θ</i> = 24.27)	99.4 (<i>θ</i> = 22.49)	98.9 (<i>θ</i> = 25.03)	99.4 (<i>θ</i> = 22.49)
Data/restraints/parameters	5117/71/421	4978/146/490	21846/1866/1652	4429/190/507
Goodness-of-fit on <i>F</i> ²	0.833	0.860	1.047	0.921
Final <i>R</i> indices [<i>I</i> > 2σ(<i>I</i>)]	<i>R</i> 1 = 0.0516, <i>wR</i> 2 = 0.1207	<i>R</i> 1 = 0.0782, <i>wR</i> 2 = 0.1611	<i>R</i> 1 = 0.0646, <i>wR</i> 2 = 0.1749	<i>R</i> 1 = 0.0471, <i>wR</i> 2 = 0.1243
<i>R</i> indices (all data)	<i>R</i> 1 = 0.0955, <i>wR</i> 2 = 0.1346	<i>R</i> 1 = 0.1686, <i>wR</i> 2 = 0.1910	<i>R</i> 1 = 0.0763, <i>wR</i> 2 = 0.1834	<i>R</i> 1 = 0.0695, <i>wR</i> 2 = 0.1325
Largest diff. peak and hole/e Å ⁻³	0.741 and −0.694	0.466 and −0.548	1.293 and −0.936	0.656 and −0.421

**Scheme 1** Synthesis of tetranuclear copper phosphonates 1–4.

(Chart 2a). However, there are important structural differences, which are discussed, below.

The electronic spectra of 1–4 reveals a broad d–d transition in the region of 680 ± 15 nm. ESI-MS spectra of 1–4 were recorded in the positive ion mode to study the stability of the tetranuclear core structures in solution. Complexes 1 and 2, which contain a pair of doubly-bridged copper(II) dimers, show major peaks at 637 nm and 659 nm corresponding to [Cu₂(μ-X)₂(μ₃-C₆H₁₁PO₃)(bpy)₄]⁺ [X = Cl (1) and CH₃COO (2)]. The ESI-MS spectra of 3 and 4 also show peaks with high nuclearity

at 889 nm [Cu₃(C₆H₁₁PO₃)(OH)₃(H₂O)(bpy)₃]⁺ and 1117 nm [Cu₃(C₆H₁₁PO₃)₂(NO₃)(C₁₂H₈N₂)₃]⁺ respectively (see ESI[†]).

Molecular structures of 1–4

The molecular structures (cationic portion only) of 1–4 are given in Fig. 1–4. Bond parameters for these compounds are summarized in the ESI.[†] The detailed supramolecular organization of these compounds is also given in the ESI.[†] The asymmetric unit of 3 contains two independent molecules (Fig. 3). The cationic part

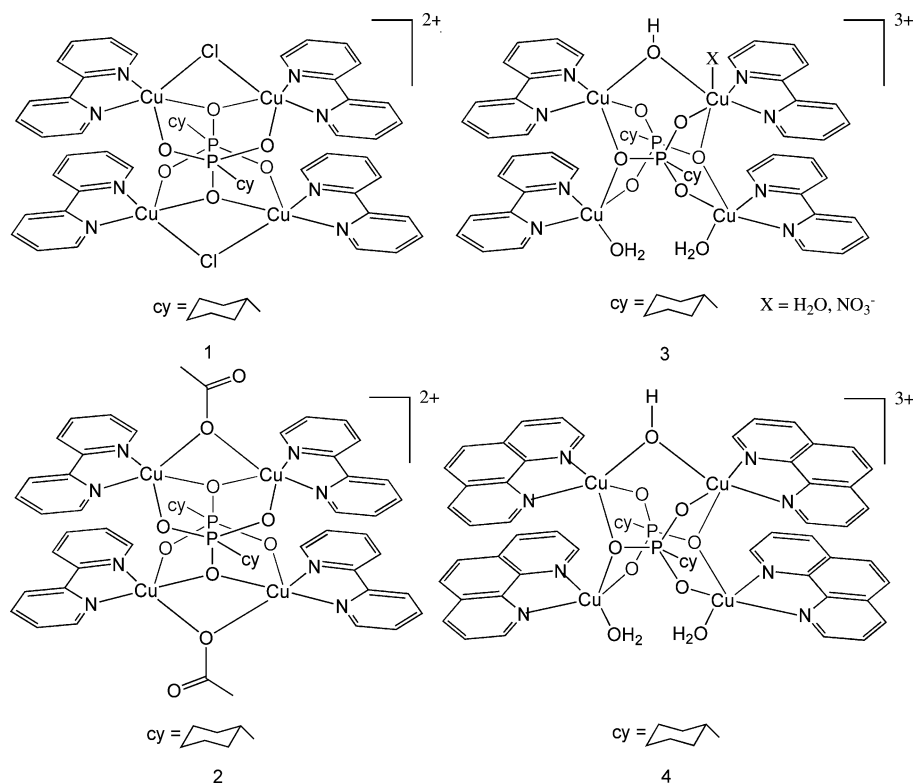


Chart 1 Cationic part of the complexes 1–4.

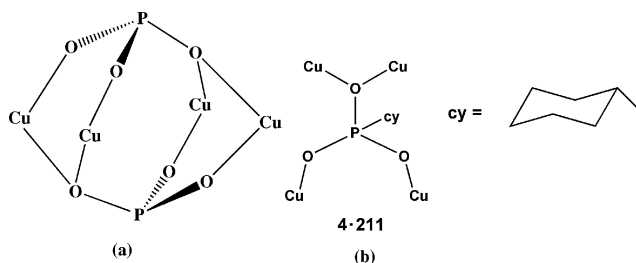


Chart 2 Tetranuclear copper unit bridged by two phosphonate groups. (b) The crystallographically established coordination modes of the cyclohexylphosphonates in the crystal structure of 1–4, and the Harris notation that describes these modes.

of the complexes 1–4 consists of a tetranuclear copper assembly. In 1 and 2 all four copper atoms are arranged in a rectangular plane while for 3 and 4 this may be described as trapezoidal. Furthermore, in 1 and 2 all four copper atoms are in the same plane (Fig. 1b and 2b). However, in 3 and 4 the tetra-copper assembly is non-planar (Fig. 3b, 3c and 4b). Mean-plane information for the tetra-copper assembly is given in Table S3 (see ESI†). In all four complexes two $[\text{C}_6\text{H}_{11}\text{PO}_3]^{2-}$ ligands are involved in holding the tetranuclear assembly together. This is accomplished by a capping tridentate coordination action by each of the phosphonate ligands (Chart 2, Fig. 2b). Two oxygen atoms of the $[\text{C}_6\text{H}_{11}\text{PO}_3]^{2-}$ ligand coordinate to two independent Cu(II) ions in a monodentate manner while the third oxygen atom is involved in bridging the remaining two Cu(II) ions. This mode of coordination can be

described as the μ_4, η^3 coordination mode or 4-211 coordination mode according to the Harris notation^{26a} (Chart 2b).

The assembly of the tetranuclear complexes of 1 and 2 is conceptually different from that for 3 and 4. Thus, the former are built from the fusion of two structurally similar symmetry-related di-copper sub-units. Both the copper atoms involved in each sub-unit are doubly-bridged: in the case of 1 by chloride and oxygen (phosphonate) atoms and in the case of 2 by oxygen atoms (acetate and phosphonate). As a result of this, symmetry-related four-membered puckered rings $[2\text{Cu}, \text{Cl}, \text{O}$ (1) and $2\text{Cu}, 2\text{O}$ (2)] are formed in these compounds (Chart 1, Fig. 1 and 2).

Furthermore, in both of these compounds, as a result of the cumulative effects of coordination, two symmetry-related six-membered rings $[2\text{Cu}, \text{P}, 2\text{O}, \text{Cl}$ (1) and $2\text{Cu}, \text{P}, 3\text{O}$ (2)] are generated within the molecular structures. The bridging chloride atoms in 1 and the acetate oxygen atoms in 2 are considerably displaced from the mean plane of the four copper atoms. Their arrangement with respect to each other can be described as *trans* (Fig. 1b and 2b). In 3 and 4 while a pair of copper atoms is bridged by $\mu\text{-OH}$ the other two have terminal ligands (H_2O) (Chart 1, Fig. 3 and 4). The presence of the single $\mu\text{-OH}$ leads to a trapezoidal arrangement of the four copper atoms in 3 and 4 while at the same time causing the assembly to be non-planar.

In view of the structural similarity of 1 and 2, the bond parameters and coordination details for these two compounds are discussed together. As mentioned (*vide supra*) the only difference between 1 and 2 is the nature of the bridging ligand. The two copper atoms present in the dicopper sub-units of 1 and 2 are five-coordinate ($2\text{N}, 2\text{O}, \text{Cl}$ for 1 and $2\text{N}, 3\text{O}$ for 2). In the case of

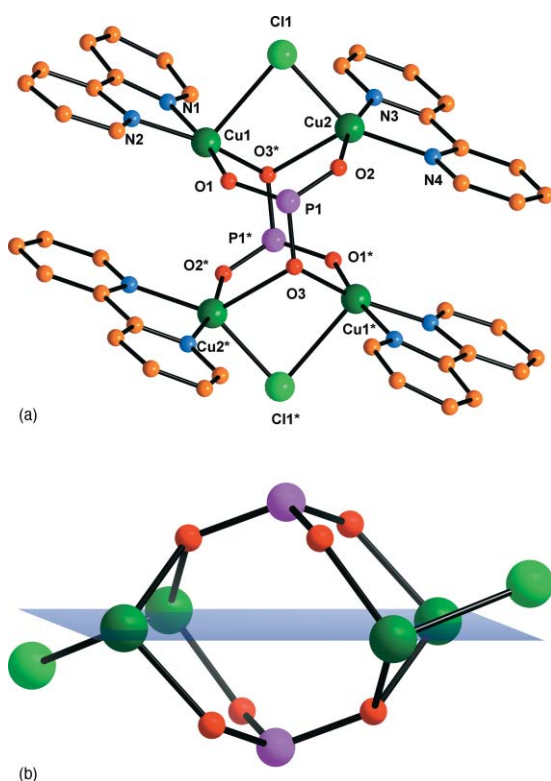


Fig. 1 (a) Cationic part of complex **1**. Cyclohexyl groups and hydrogen atoms have been removed for the sake of clarity. (b) View of the tetranuclear core of **1**. The bridging chloride atoms are displaced from the mean plane of the four copper atoms by 0.76 Å.

1, Cu1 is in a square pyramidal geometry ($\tau = 0.035$; basal plane is made up of 2N and 2O, Cl is present in the apical position) while Cu2 is in a distorted trigonal bipyramidal geometry ($\tau = 0.707$).^{26b} The axial bond angle in the latter (Cl1–Cu2–N4) is 150.23°. In a slight variation, in **2**, both Cu1 and Cu2 are present in a near square pyramidal geometry [$\tau = 0.068$ (Cu1); $\tau = 0.105$ (Cu2)]. The bond distances within the four-membered sub-unit are not equal. Thus in **1**, the Cu1–Cl1 distance is 2.707(2) Å while Cu2–Cl1 is 2.3520(19) Å. Similarly Cu1–O3* is 1.969(4) Å and Cu2–O3* is 2.396(4) Å. A similar situation is also found in **2** (see ESI†). The Cu–O distances involving a μ -O (phosphonate) are longer in comparison to the bond distances observed where a monodentate oxygen atom is involved in coordination (see ESI†). The rectangular arrangement of the copper atoms in these assemblies is gauged by the near perfect planarity of the tetra-nuclear array (see ESI†) and the intramolecular copper distances. Thus, the shortest Cu–Cu edge distances in **1** and **2** are 3.338 Å (Cu1–Cu2) and 3.255 Å (Cu1–Cu2*) respectively. The corresponding longer edge distances (Cu1–Cu2*) are 4.047 and 4.138 Å. The coordination environments of the copper atoms in **3** and **4** are similar except that the nitrogenous chelating ligand in the former is 2,2'-bipyridine while in the latter it is 1,10-phenanthroline (Chart 1, Fig. 3 and 4). In **4** all the copper atoms are five-coordinate and in a square pyramidal geometry with a 2N,3O coordination environment. The asymmetric unit of **3** contains two molecules. In both of these, three of the four copper atoms are five-coordinate and square pyramidal; the fourth copper atom is six-coordinate with an additional water or nitrate ligand (Fig. 3).

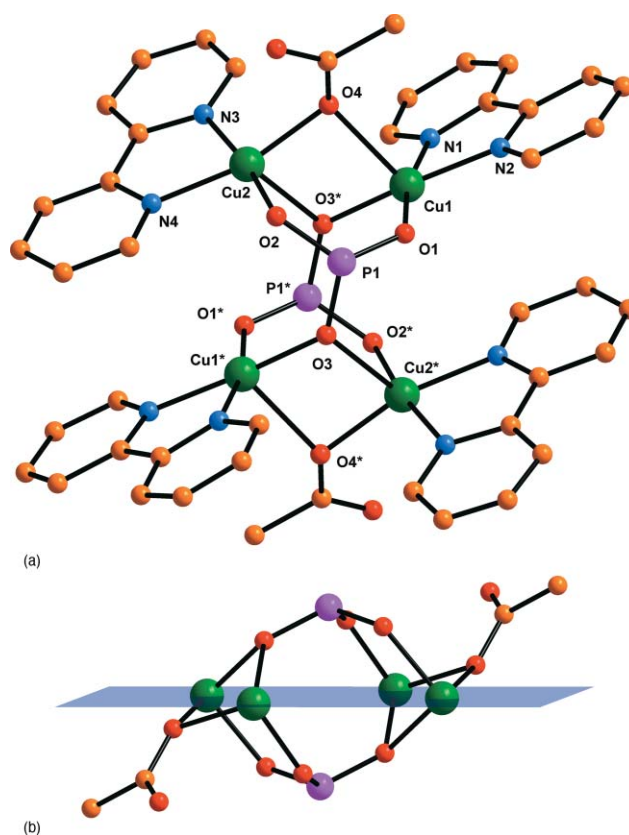
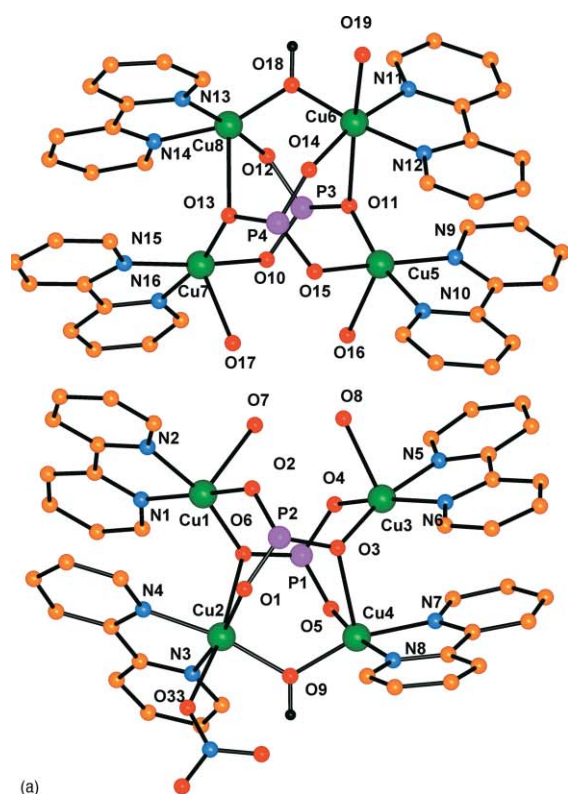


Fig. 2 (a) Cationic part of **2**. Cyclohexyl groups and hydrogen atoms have been removed for the sake of clarity. (b) View of the tetranuclear copper core. The bridging oxygen atoms of the acetate ligand are displaced by 0.55 Å from the mean plane of the copper atoms.

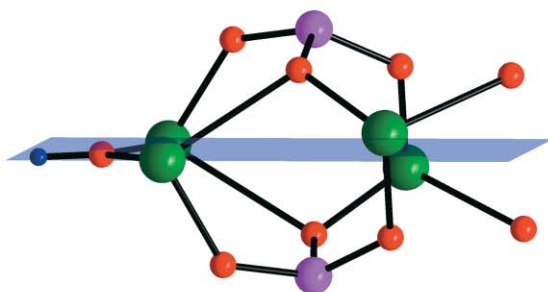
Compounds **3** and **4** do not contain doubly-bridged copper atoms as found in **1** and **2**. However, two copper centres are bridged symmetrically by a μ -OH. The Cu–O distances involved are: for **3**, Cu2–O9 (1.925(4) Å) and Cu4–O9 (1.886(4) Å); for **4**, Cu1–O4 1.906 (3) Å. The phosphonate coordination to the four copper centres is tripodal. One of the oxygen atoms is involved in a bridging coordination while the other two are involved in monodentate coordination. The Cu–O bond distances observed for **3** and **4** with the phosphonate ligand indicate the highly unsymmetrical nature of the bridging coordination (see ESI†). For example, in **4** the Cu1–O1 bond distance is 2.428(4) Å while the Cu2–O1 distance is 1.961(4) Å. One possible reason for this is the trapezoidal arrangement of the four copper centres in these assemblies. Accordingly, in **3** and **4**, four different inter-copper distances are observed (see ESI†).

Comparison of the structural features of 1–4 with related systems

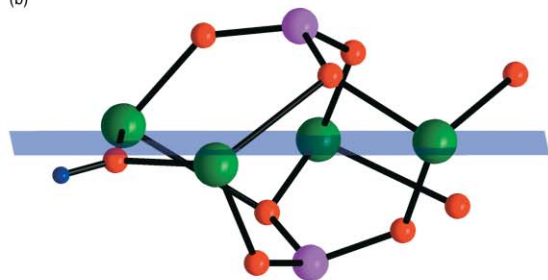
Tetranuclear copper clusters containing phosphate ligands are more predominant in comparison to those involving phosphonates.²⁷ In this discussion we restrict ourselves only to tetranuclear copper phosphonates. The tetranuclear copper cores found in **1–4** are shown in Chart 3. As discussed (*vide supra*) two types of cores are found in these compounds. Compounds **1** and **2** possess a *closed* type of core where two dimeric [Cu₂(μ -X)(μ -O)] units are interlinked with each other (Chart 3, Type A). The phosphonate ligand is involved in connecting the two dimers



(a)



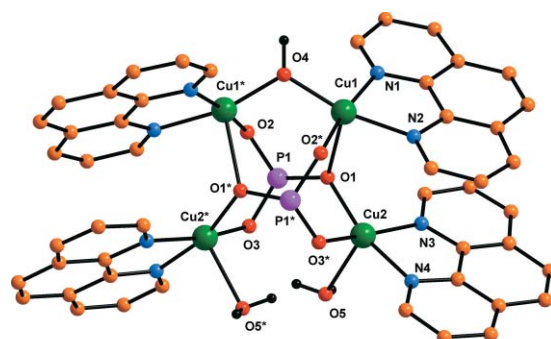
(b)



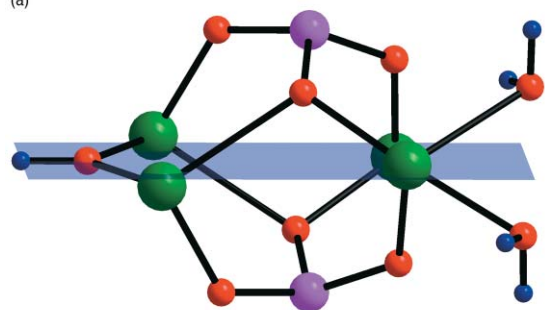
(c)

Fig. 3 (a) Cationic part of the two independent molecules present in the asymmetric unit of **3**. Cyclohexyl groups and hydrogen atoms have been removed for clarity. (b) View of the non-planar tetra-copper core (Cu1, Cu2, Cu3 and Cu4) of upper molecule shown in Fig. 3(a). (c) View of the non-planar tetra-copper core of lower molecule shown in Fig. 3(a) (Cu5, Cu6, Cu7 and Cu8).

together. While one oxygen atom of a phosphonate forms the μ -O linking Cu_a and Cu_b, the other two oxygen atoms are monodentate and bind to Cu_c and Cu_d. As noted above, the tetranuclear cores



(a)



(b)

Fig. 4 (a) Cationic part of **4**. Cyclohexyl groups and hydrogen atoms have been removed for clarity. (b) View of the non-planar tetra-copper core of **4**.

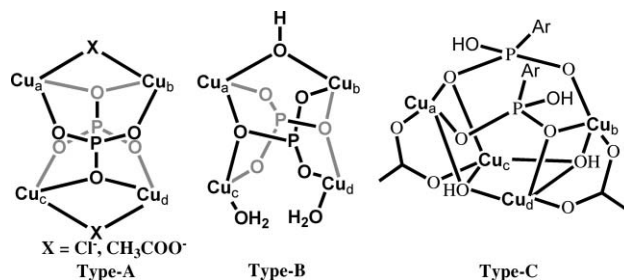


Chart 3 Three representative framework structures of tetranuclear copper(II) phosphonate assemblies formed by using ancillary nitrogenous ligands.

of **3** and **4** have a different structural arrangement. These contain more *open* cores. Thus, two copper atoms (a and b) are linked to each other by a μ -OH. The other two copper atoms (c and d) are not bridged to each other but instead have a terminal water ligand each (Chart 3, Type B). The connectivity of the four copper atoms is established again by two tripodal phosphonates, which act slightly differently. However, one of the oxygen atoms of the phosphonate ligand binds Cu_a and Cu_c in a μ bridging mode while the other two coordinate in a unidentate manner to bind Cu_b and Cu_d. The coordination mode of the phosphonate ligand is twisted by 90° for **3** and **4** in comparison to **1** and **2**. There are only two other tetranuclear copper(II) phosphonates containing ancillary ligands, to the best of our knowledge. Both of these have been reported from our laboratory. One of these is $[\text{Cu}_2(\mu\text{-Cl})(\mu_3\text{-MePO}_3)(\text{Cl})(3,5\text{-Me}_2\text{PzH})_2]_2$ which is obtained in an indirect desulfurization/hydrolysis reaction involving $\text{MeP}(\text{S})(3,5\text{-Me}_2\text{Pz})_2$ and CuCl_2 .

The tetranuclear core of this compound corresponds to Type A found in the present instance, although within a dimeric pair the disposition of the ancillary ligands is not symmetric as

is the situation in the present instance. The other tetranuclear copper phosphonate known in literature, $[\text{Cu}_4(\mu\text{-OH})_2(\text{ArP}(\text{O})_2\text{-OH})_2(\text{CH}_3\text{CO}_2)_2(\text{DMPZH})_4][\text{CH}_3\text{COO}]_2$ has been obtained in the reaction involving $\text{Cu}(\text{CH}_3\text{COO})_2\cdot\text{H}_2\text{O}$ with $\text{ArP}(\text{O})(\text{OH})_2$ ($\text{Ar} = 2,4,6\text{-iPr-C}_6\text{H}_3$). In this compound, the tetranuclear copper assembly is an asymmetric cage containing three continuous four-membered rings, $[\text{Cu}_2(\mu\text{-O})(\mu\text{-OH})]$, $[\text{Cu}(\mu\text{-OH})_2]$ and $[\text{Cu}_2(\mu\text{-O})(\mu\text{-OH})]$. Bridging ligands in the form of $[\text{ArP}(\text{O})_2(\text{OH})]^-$ and CH_3COO^- hold the cage together (Type C, Chart 3). The important difference between Type C cores *vis-à-vis* the Type A and B cores lies in the fact that one of the oxygen atoms of the $[\text{ArP}(\text{O})_2(\text{OH})]^-$ ligand in the former is not involved in coordination. Because of this, the phosphinate ligand holds three copper atoms together in contrast to the situation in Type A and Type B structures where four copper atoms are bound by a capping phosphonate ligand (Chart 3). The metric parameter variations in these three structural types are not very significant. For example the average $\text{Cu-O}(\eta^1)$ and $\text{Cu-O}(\mu_3)$ distances in $[\text{Cu}_2(\mu\text{-Cl})(\mu_3\text{-MePO}_3)(\text{Cl})(3,5\text{-Me}_2\text{PzH})_3]_2$ are 2.003(5) and 1.990(4) Å respectively, which are comparable to the situation found in compounds **1–4**. Also, as found in **1** and **2**, the four copper atoms in $[\text{Cu}_2(\mu\text{-Cl})(\mu_3\text{-MePO}_3)(\text{Cl})(3,5\text{-Me}_2\text{PzH})_3]_2$ lie in a single plane.

Magnetic studies

Magnetic measurements indicate that all the presented compounds (**1–4**) exhibit moderately strong antiferromagnetic intramolecular coupling between the spin-1/2 Cu(II) centres resulting in singlet ground states.

The local symmetry of the central $\text{Cu}_4(\text{PO}_3)_2(\mu\text{-X})_n$ core ($\text{X} = \text{O}, \text{Cl}; n = 1, 2$) suggests the following superexchange connectivities for a Heisenberg exchange model (Fig. 5): two types of exchange pathways for compound **1** (where J_1 involves a phosphonate μ_3 -oxo centre, an O–P–O bridge and a bridging chloride, J_2 involves two O–P–O pathways) and **2** (where J_1 involves a phosphonate μ_3 -oxo centre, an O–P–O bridge and a bridging acetate oxo centre, J_2 as in compound **1**) and four exchange pathways for compounds **3** and **4** (J_1 : two O–P–O bridges and a μ -hydroxo group, J_2 : an O–P–O bridge and a phosphonate μ_3 -oxo centre, J_3 : two O–P–O bridges) (see Fig. 5).

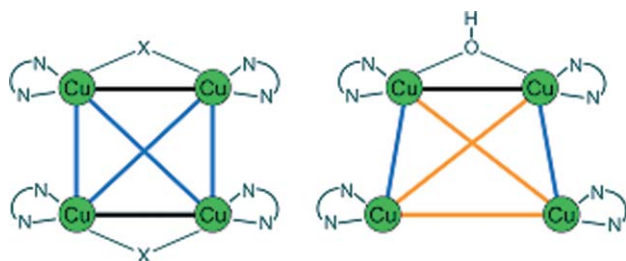


Fig. 5 Exchange coupling scheme for compounds **1** (left), **2** (left), **3** (right) and **4** (right), using the same perspectives as Chart 1. The effective exchange pathways are represented by bold bonds: J_1 black, J_2 blue, J_3 orange. Corresponding isotropic Heisenberg spin Hamiltonians: $\text{H} = -J_1(\text{S1S2} + \text{S3S4}) - J_2(\text{S1S3} + \text{S1S4} + \text{S2S3} + \text{S2S4})$ (for **1** and **2**); $\text{H} = -J_1(\text{S1S2}) - J_2(\text{S1S4} + \text{S2S3}) - J_3(\text{S1S3} + \text{S2S4} + \text{S3S4})$ (for **3** and **4**).

Note that these models are simplified in that small variations in the exact local geometries of the Cu-O-P-O-Cu fragments are assumed to have no significant impact on the resulting

contributions to the overall exchange energies that depend on such bridges. Whereas the types of exchange pathways are identical in nature for compounds **3** and **4**, the difference in the terminal (bridging N-donor ligands (bpy for **3**, phen for **4**) slightly affects the geometry of the exchange pathways in the $\text{Cu}_4(\text{PO}_3)_2(\mu\text{-OH})$ cores.

Correspondingly, the experimental susceptibility curves for **3** and **4** differ only slightly (below approx. 100 K). Furthermore, the presence of two crystallographically distinct core geometries in compound **3** (with planar and non-planar Cu_4 arrangements, see Fig. 3) complicates the magnetic analysis since the exchange energies cannot be unambiguously assigned to the two species involved, effectively limiting the interpretation of bulk susceptibility data for these mixed species. Since the coordination environments of all Cu(II) centres in compounds **1** to **4** are approximately square pyramidal (with minor deviations from the square *cis*- $\text{N}_2\text{O}_2/\text{N}_2\text{OCl}$ coordination plane (see ESI†) with an elongated axial bond, *i.e.* Jahn–Teller-distorted as is typical for these d^9 systems, the g tensors can in a first approximation be characterized by the axial and perpendicular components g_z and g_x/g_y , respectively. Using uniform typical values of $g_z = 2.30$ and $g_x = g_y = 2.05$, least-squares fits to the experimental susceptibility data sets (Fig. 6 and 7) were performed based on the simplified isotropic model. Heisenberg spin operators as defined in Fig. 5. These models yielded the following effective, all-antiferromagnetic exchange energies: **1**: $J_1/k_B = -6.2$ K, $J_2/k_B = -5.8$ K; **2**: $J_1/k_B = -6.8$ K, $J_2/k_B = -6.3$ K; **4**: $J_1/k_B = -18.4$ K, $J_2/k_B = -9.2$ K, $J_3/k_B = -6.4$ K. As stated above, the mixture of core geometries in **3** prevented such fitting procedure; a qualitative comparison between the susceptibility *vs.* temperature curves of **3** and **4** (Fig. 7) indicates that the overall antiferromagnetic coupling observed in **3** should be slightly weaker.

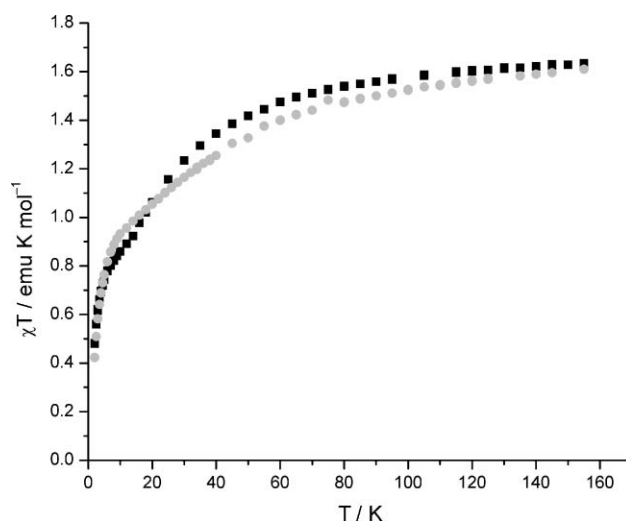


Fig. 6 Experimental temperature dependence of χT for compounds **1** (0.1 tesla, left, grey circles) and **2** (0.1 tesla, left, black squares).

Overall these exchange constants are slightly smaller than for the comparable phosphonate-bridged polynuclear Cu(II) species, probably due to the relatively large Cu–Cu distances obtained in the presented cluster compounds.²⁸

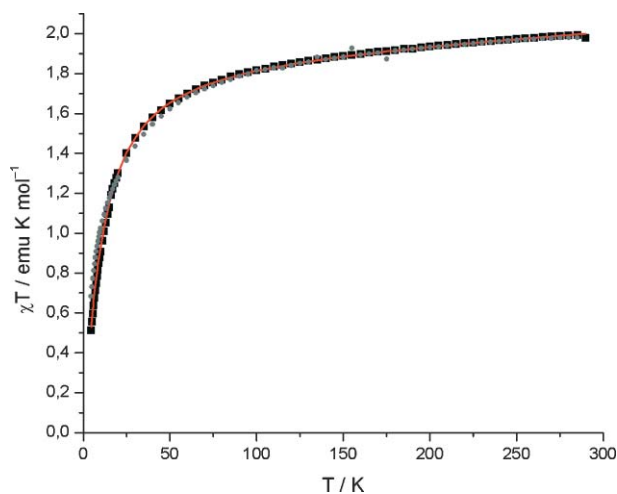


Fig. 7 Experimental temperature dependence of χT for compounds **3** (0.5 tesla, right, grey circles), and **4** (0.5 tesla, right, black squares) and representative least-squares fit to the proposed Heisenberg model for **4** (red graph). Note the different scale to Fig. 6.

Cleavage of plasmid DNA

We have systematically examined the DNA cleavage ability²⁹ of complexes **1–4** (Fig. 8). Time-course experiments reveal that **1** and **3** were able to mediate complete conversion of the supercoiled pBR322 DNA form I to nick form II in 120 min (Fig. 5). In contrast, only partial conversion occurred in the presence of **2** (50%) and **4** (40%). To foster the reaction we have added magnesium monoperoxyphthalate (MMPP). In all cases, we observed rapid conversion of the supercoiled pBR322 DNA form I to form II within 2 min (Fig. 9).

DNA cleavage mechanism

Copper-based artificial nucleases function through oxidative and/or hydrolytic pathways. In view of this, we probed the cleavage

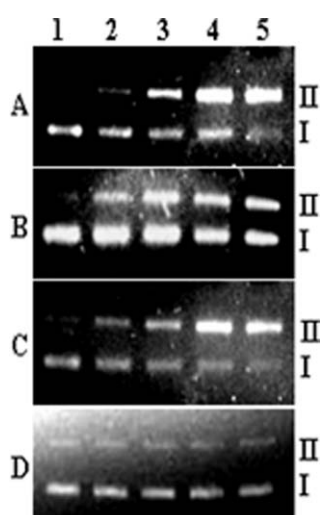


Fig. 8 Time-course experiment for the conversion of supercoiled pBR322 DNA form I to nick form II in the presence of **1–4** at different time intervals (complex **1** corresponds to gel A, **2** to gel B, **3** to gel C and **4** to gel D). Lane 1: DNA alone; lanes 2–5: DNA + complexes (30, 60, 90 and 120 min respectively).

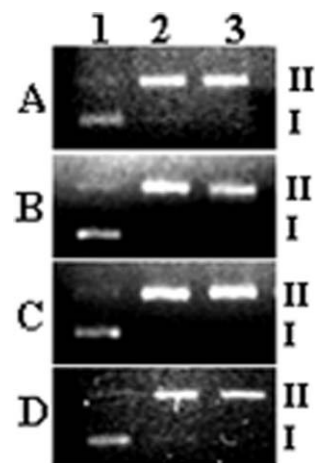


Fig. 9 pBR322 DNA cleavage by **1–4** in the presence of MMPP (complex **1** corresponds to gel A, **2** to gel B, **3** to gel C and **4** to gel D) at different time intervals. Lane 1: DNA alone; lanes 2–3: DNA + complex + MMPP.

mechanism of **1–4**. In the presence of EDTA, the cleavage reaction is completely inhibited demonstrating the crucial role of copper in plasmid modification. Hydroxyl radical scavengers, dimethyl sulfoxide (DMSO), D-mannitol or *tert*-butylalcohol do not inhibit cleavage reactions, demonstrating that radicals are not involved in the cleavage process. On the other hand, NaN_3 is a well-known quencher of singlet oxygen.

This suggests that *in situ* generation and possible involvement of singlet oxygen is involved in the plasmid cleavage (Fig. 10). However, the hydrolytic pathway for plasmid modification also appears potent in the current instance as demonstrated by the fact that DNA cleavage does not decrease under anaerobic conditions (Fig. 11). Thus, it appears that both multiple reaction pathways involving singlet oxygen³⁰ as well as hydrolysis are involved in the plasmid cleavage activity mediated by **1–4**.

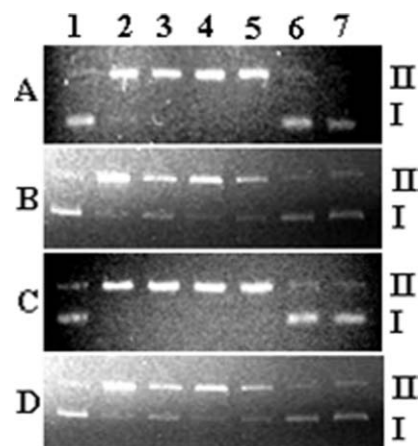


Fig. 10 pBR322 cleavage experiments involving **1–4** in the presence of free radical scavengers and singlet oxygen quencher assisted by the complexes (complex **1** corresponds to gel A, **2** to gel B, **3** to gel C and **4** to gel D) in a 2 min reaction. Lane 1: DNA alone; lane 2: pBR322 + complex + MMPP; lane 3: pBR322 + complex + MMPP + DMSO; lane 4: pBR322 + complex + MMPP + D-mannitol; lane 5: pBR322 + complex + MMPP + *t*-BuOH; lane 6: pBR322 + complex + MMPP + EDTA; lane 7: pBR322 + complex + MMPP + NaN_3 .

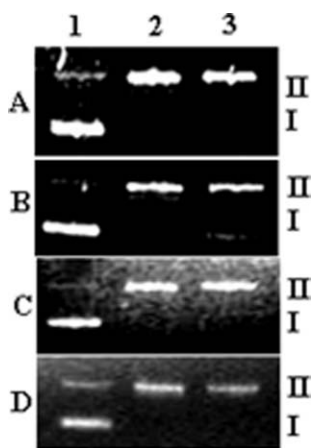


Fig. 11 pBR322 DNA cleavage in anaerobic conditions by 1–4 (complex 1 corresponds to gel A, 2 to gel B, 3 to gel C and 4 to gel D) at different time intervals. Lane 1: DNA alone; lanes 2–3: DNA + complex + MMPP.

Conclusion

We have synthesized four tetranuclear copper(II) phosphonate cages (1–4) in three-component reactions involving a Cu(II) salt, an ancillary ligand such as 2,2'-bipyridine and cyclohexylphosphonic acid. In all the cases two phosphonate ligands act as bicipping ligands and hold the four copper atoms together in a tridentate coordination action. The role of the chelating ligand is also crucial. It blocks two coordination positions around copper and reduces the chances of other side-products. The magnetic studies on these complexes reveal an overall anti-ferromagnetic behaviour. The metal phosphonates 1–4 also show impressive plasmid cleavage activity.

Acknowledgements

We thank the Council of Scientific and Industrial Research (CSIR), New Delhi, India and the Department of Science and Technology, India for financial support. VC is thankful to IIT Kanpur for the Lalit Kapoor Chair Professorship. TS, PT and RA thank IIT Kanpur and CSIR for fellowships. AS thanks the EPSRC (Engineering and Physical Sciences Research Council), U. K. for financial support.

Notes and references

- (a) A. Clearfield, *Progress in Inorganic Chemistry: Metal–Phosphonate Chemistry*, ed. K. D. Karlin, John Wiley & Sons, New York, 1998, vol. 47, p. 371, and references therein; (b) G. Cao, H.-G. Hong and T. E. Mallouk, *Acc. Chem. Res.*, 1992, **25**, 420; (c) A. Clearfield, *Curr. Opin. Solid State Mater. Sci.*, 2002, **6**, 495; (d) A. Clearfield, *Curr. Opin. Solid State Mater. Sci.*, 1996, **1**, 268; (e) M. E. Thompson, *Chem. Mater.*, 1994, **6**, 1168–1175; (f) A. Subbiah, D. Pyle, A. Rowland, J. Huang, A. R. Narayanan, P. Thiyagarajan, J. Zoń and A. Clearfield, *J. Am. Chem. Soc.*, 2005, **127**, 10826; (g) S.-Y. Song, J.-F. Ma, J. Yang, M.-H. Cao and K.-C. Li, *Inorg. Chem.*, 2005, **44**, 2140; (h) W. Ouellette, M. H. Yu, C. J. O'Connor and J. Zubieta, *Inorg. Chem.*, 2006, **45**, 7628; (i) W. Ouellette, M. H. Yu, C. J. O'Connor and J. Zubieta, *Inorg. Chem.*, 2006, **45**, 3224; (j) E. Burkholder, V. Golub, C. J. O'Connor and J. Zubieta, *Inorg. Chem.*, 2004, **43**, 7014; (k) B.-P. Yang and J.-G. Mao, *Inorg. Chem.*, 2005, **44**, 566.
- (a) A. Clearfield, *Inorganic Ion Exchange Materials*, CRC Press, Boca Raton, Florida, 1982; (b) G. Alberti, in *Comprehensive Supramolecular Chemistry*, ed. G. Alberti and T. Bein, Pergamon, New York, 1996, vol.

- p. 151; (c) J. D. Wang, A. Clearfield and G.-Z. Peng, *Mater. Chem. Phys.*, 1993, **35**, 208; (d) B. Zang and A. Clearfield, *J. Am. Chem. Soc.*, 1997, **119**, 2751.
- (a) F. Fredoueil, D. Massiot, P. Janvier, F. Gingl, M. Bujoli-Doeuff, M. Evian, A. Clearfield and B. Bujoli, *Inorg. Chem.*, 1999, **38**, 1831; (b) K. Maeda, Y. Kiyozumi and F. Mizukami, *J. Phys. Chem. B*, 1997, **101**, 4402; (c) Q. Yue, J. Yang, G.-H. Li, G.-D. Li and J.-S. Chen, *Inorg. Chem.*, 2006, **45**, 4431; (d) L. A. Gallagher, S. A. Serron, X. Wen, B. J. Hornstein, D. M. Dattelbaum, J. R. Schoonover and T. J. Meyer, *Inorg. Chem.*, 2005, **44**, 2089; (e) K. Maeda, *Microporous Mesoporous Mater.*, 2004, **73**, 47.
- (a) B.-Z. Wan, R. G. Anthony, G.-Z. Peng and A. Clearfield, *J. Catal.*, 1994, **19**, 101; (b) D. Deniaud, B. Schollorn, J. Mansury, J. Rouxel, P. Battion and B. Bujoli, *Chem. Mater.*, 1995, **7**, 995; (c) A. Hu, H. Ngo and W. Lin, *J. Am. Chem. Soc.*, 2003, **125**, 11490; (d) A. Hu, G. T. Yee and W. Lin, *J. Am. Chem. Soc.*, 2005, **127**, 12486; (e) G. Nonglaton, I. O. Benitez, I. Guisle, M. Pipeler, J. Leger, D. Dubreuil, C. Tellier, D. R. Talham and B. Bujoli, *J. Am. Chem. Soc.*, 2004, **126**, 1497.
- (a) S. B. Ungashe, W. L. Wilson, H. E. Katz, G. R. Scheller and T. M. Putvinski, *J. Am. Chem. Soc.*, 1992, **114**, 8717; (b) M. J. Sanchez-Moreno, A. Fernandez-Botello, R. B. Gomez-Coca, R. Griesser, J. Ochocki, A. Kotynski, J. Niclos-Gutierrez, V. Moreno and H. Sigel, *Inorg. Chem.*, 2004, **43**, 1311; (c) Z.-Y. Du, H.-B. Xu and J.-G. Mao, *Inorg. Chem.*, 2006, **45**, 6424.
- (a) A. Cabeza, M. A. G. Aranda, S. Bruque, D. M. Poojary, A. Clearfield and J. Sanz, *Inorg. Chem.*, 1998, **37**, 4168; (b) B. Zhang, D. M. Poojary and A. Clearfield, *Inorg. Chem.*, 1998, **37**, 249; (c) P. Ayyappan, O. R. Evans, Y. Cui, K. A. Wheeler and W. Lin, *Inorg. Chem.*, 2002, **41**, 4978.
- Yu. Yang, M. G. Walawalkar, J. Pinkas, H. W. Roesky and H.-G. Schmidt, *Angew. Chem., Int. Ed.*, 1998, **37**, 96.
- V. Baskar, M. Shanmugam, E. C. Sañudo, M. Shanmugam, D. Collison, E. J. L. McInnes, Q. Wei and R. E. P. Winpenny, *Chem. Commun.*, 2007, 37.
- G. Anantharaman, M. G. Walawalkar, R. Murugavel, B. Gábor, H.-I. Regine, M. Baldus, B. Angerstein and H. W. Roesky, *Angew. Chem., Int. Ed.*, 2003, **42**, 4482.
- G. Anantharaman, V. Chandrasekhar, M. G. Walawalkar, H. W. Roesky, D. Vidovic, A. J. Magull and M. Noltemeyer, *Dalton Trans.*, 2004, 1271.
- Y. Yang, H.-G. Schmidt, M. Noltemeyer, J. Pinkas and H. W. Roesky, *J. Chem. Soc., Dalton Trans.*, 1996, 3609.
- H.-C. Yao, Y.-Z. Li, Y. Song, Y.-S. Ma, L.-M. Zheng and X.-Q. Xin, *Inorg. Chem.*, 2006, **45**, 59.
- H.-C. Yao, Y.-Z. Li, L.-M. Zheng and X.-Q. Xin, *Inorg. Chim. Acta*, 2005, **358**, 2523.
- P. Yin, Y. Peng, L.-M. Zheng, S. Gao and X.-Q. Xin, *Eur. J. Inorg. Chem.*, 2003, 726.
- R. Murugavel and S. Shanmugam, *Chem. Commun.*, 2007, 1257.
- V. Chandrasekhar, V. Baskar, A. Steiner and S. Zacchini, *Organometallics*, 2002, **21**, 4528.
- V. Chandrasekhar and S. Kingsley, *Angew. Chem., Int. Ed.*, 2000, **39**, 2320.
- V. Chandrasekhar, S. Kingsley, A. Vij, K. C. Lam and A. L. Rheingold, *Inorg. Chem.*, 2000, **39**, 3238.
- V. Chandrasekhar, S. Kingsley, B. Hatigan, M. K. Lam and A. L. Rheingold, *Inorg. Chem.*, 2002, **41**, 1030.
- V. Chandrasekhar, P. Sasikumar, R. Boomishankar and G. Anantharaman, *Inorg. Chem.*, 2006, **45**, 3344.
- V. Chandrasekhar, L. Nagarajan, K. Gopal, V. Baskar and P. Kögerler, *Dalton Trans.*, 2005, 3143.
- R. Murugavel, P. Davis and M. G. Walawalkar, *Z. Anorg. Allg. Chem.*, 2005, **631**, 2806.
- B. S. Furniss, A. J. Hannaford, P. W. G. Smith and A. R. Tatchell, *Vogel's Textbook of Practical Organic Chemistry*, 5th edn, Longman, London, 1989.
- J. J. Borrás-Allmenar, J. J. Clemente, E. Coronado and B. S. Tsukerblat, *Comput. Chem.*, 2001, **22**, 985.
- G. M. Sheldrick, *SHELXL-97, Program for refinement of crystal structures*, University of Göttingen, Germany, 1997.
- (a) R. A. Coxall, S. G. Harris, S. Henderson, S. Parsons, R. A. Taskar and R. E. P. Winpenny, *J. Chem. Soc., Dalton Trans.*, 2000, **14**, 2349; (b) A. W. Addison, T. N. Rao, J. Reedijk, J. V. Rijn and G. C. Verschoor, *J. Chem. Soc., Dalton Trans.*, 1984, 1349.

- 27 (a) R. P. Doyle, P. E. Kruger, B. Moubaraki, K. S. Murray and M. Nieuwenhuyzen, *Dalton Trans.*, 2003, 4230; (b) M. Kato and T. Tanase, *Inorg. Chem.*, 2005, **44**, 8; (c) S. Youngme, P. Phuengphai, N. Chaichit, G. A. van Albada, O. Roubeau and J. Reedijk, *Inorg. Chim. Acta*, 2005, **358**, 849; (d) S. Youngme, P. Phuengphai, N. Chaichit, G. A. van Albada, O. Roubeau and J. Reedijk, *Inorg. Chim. Acta*, 2005, **358**, 2262.
- 28 V. Baskar, M. Shanmugam, E. C. Sañudo, M. Shanmugam, D. Collison, E. J. L. McInnes, Q. Wei and R. E. P. Winpenny, *Chem. Commun.*, 2007, 37.
- 29 (a) S. G. Srivatsan, M. Parvez and S. Verma, *J. Inorg. Biochem.*, 2003, **97**, 340; (b) V. Chandrasekhar, P. Deria, V. Krishnan, A. Athimoolam, S. Singh, C. Madhavaiah, S. G. Srivatsan and S. Verma, *Bioorg. Med. Chem. Lett.*, 2004, **14**, 1559; (c) V. Chandrasekhar, S. Nagendran, R. Azhakar, R. M. Kumar, A. Srinivasan, K. Ray, T. K. Chandrashekar, C. Madhavaiah, S. Verma, U. D. Priyakumar and N. G. Sastry, *J. Am. Chem. Soc.*, 2005, **127**, 2410; (d) V. Chandrasekhar, A. Athimoolam, V. Krishnan, R. Azhakar, C. Madhavaiah and S. Verma, *Eur. J. Inorg. Chem.*, 2005, **8**, 1482; (e) C. Madhavaiah and S. Verma, *Chem. Commun.*, 2003, **6**, 800; (f) S. Das, C. Madhavaiah, S. Verma and P. K. Bharadwaj, *Inorg. Chim. Acta*, 2005, **358**, 3236; (g) L. M. Pope, K. A. Reich, D. R. Graham and D. S. Sigman, *J. Biol. Chem.*, 1982, **257**, 12121; (h) J. Sankar, H. Rath, V. Prabhuraja, S. Gokulnath, T. K. Chandrashedkar, C. S. Purohit and S. Verma, *Chem.–Eur. J.*, 2006, **13**, 105.
- 30 (a) A. Fortner, S. Wang, G. K. Darbha, A. Ray, H. Yu, P. C. Ray, R. R. Kalluru, C. K. Kim, V. Rai and J. P. Singh, *Chem. Phys. Lett.*, 2007, **434**, 127; (b) B. Macias, M. V. Villa, F. Sanz, J. Borrás, M. Gonzalez-Alvarez and G. Alzuet, *J. Inorg. Biochem.*, 2005, **99**, 1441; (c) A. K. Patra, S. Dhar, M. Nethaji and A. R. Chakravarty, *Chem. Commun.*, 2003, **13**, 1562; (d) Y. Li and M. A. Trush, *Carcinogenesis*, 1993, **14**, 1303.